

# Density dependence in the thermal conductivity of cellulose fiber mats and wood shavings mats: investigation of the apparent thermal conductivity of coarse pores

Noboru Sekino<sup>1</sup>

Received: 12 May 2015 / Accepted: 6 October 2015 / Published online: 3 November 2015  
© The Japan Wood Research Society 2015

**Abstract** Thermal conductivities ( $k$ -values) of cellulose fiber (CF) and wood shavings (WS) mats were measured, and the density dependence of  $k$ -values in the ranges 28–60 and 60–100 kg/m<sup>3</sup> for CF mats and WS mats, respectively, was investigated. The  $k$ -value of the CF mats tended to increase with increasing mat density, but that of the WS mats showed a much weaker relationship. In order to discuss this density dependence in  $k$ -values, the apparent thermal conductivity ( $k_{cp}$ ) of coarse pores in the mats, which includes the effects of convective and radiant heat transfer, was calculated. The results revealed that the density dependence in the  $k$ -values of the CF mats derived only from an increase in the number of heat bridges, consisting of fibers and their contact points. Also, the smaller density dependence of the  $k$ -values of the WS mats than that of the CF mats was found to be explicable by the density dependence of  $k_{cp}$  in the WS mats, because a lower  $k_{cp}$  at higher mat densities contributes to the lowering of mat thermal conductivity in a way that balances the increase in heat bridges as mat density increases.

**Keywords** Thermal conductivity · Coarse pores · Cellulose fiber mat · Wood shavings mat · Convective heat transfer

## Introduction

Reducing energy consumption of buildings is required in order to counteract global warming induced by carbon dioxide, and thermal insulation of a building is an important part of this process. One of the development concepts used in the design of insulation materials is to aim to achieve a low thermal conductivity ( $k$ -value). High-performance products such as phenol foams and glass wool made of very fine fibers have become popular lately; their  $k$ -values range from 0.020 to 0.040 W/(mK) [1]. Recently initiated work on vacuum insulation panels (VIPs) is aiming for a much lower  $k$ -value. For instance, Kwon et al. [2] reported a theoretical investigation on the thermal transport mechanisms of VIPs. Technology that achieves a low  $k$ -value is very important because it makes it possible to make insulation materials that are thinner than conventional ones, which results in saving valuable space in a building.

An alternative development concept is to aim to use environmentally friendly products. One aspect of being environmentally friendly is effective utilization of unused resources. Using agricultural wastes, forest product wastes, textile wastes, and so on, as the raw materials of thermal insulation products is favorable for working towards a sustainable society based on resource recycling. For instance, Binici et al. [3] investigated the  $k$ -value of fiber mats made of sunflower stalks, Zhou et al. [4] reported a  $k$ -value for binderless cotton stalk fiberboards, and Yamauchi et al. [5] published a  $k$ -value for thick insulation panels made from sugi (*Cryptomeria japonica* D. Don) bark and used as a floor heating base material. The  $k$ -values of these insulation materials range from 0.050 to 0.073 W/(mK) because their density is more than 150 kg/m<sup>3</sup>. Although these  $k$ -values are greater than (i.e., inferior to) that of the glass wool commonly used in buildings, the materials are nevertheless fully usable, as long as a

Parts of this report were presented at the 62nd Annual Meeting of the Japan Wood Research Society, Sapporo, March 2012.

✉ Noboru Sekino  
sekino@iwate-u.ac.jp

<sup>1</sup> Faculty of Agriculture, Iwate University, Morioka 020-8550, Japan

building has space to accommodate thick insulation materials. The other environmentally friendly aspect to consider is the energy consumption involved in production of the materials. Most thermal insulation materials require a heating process in their manufacturing line. Based on both of these aspects, cellulose fiber (CF) is an advantageous insulation material because it is made of waste newspapers and does not require a heating process.

Similarly, wood shavings (WS) are a potential raw material for insulation. WS that are created as processing waste during the production of dry timber are especially favorable, since they do not require a drying process. Kawamura et al. [6, 7] reported a manufacturing technology for WS binderless insulation panels (WSBIPs) in which an extruding-type mat-forming method was employed without a heating process. Sekino et al. [8, 9] investigated the heat storage capacity and fire resistance of full-scale thick WSBIPs. The  $k$ -value of WSBIPs with a density of  $100 \text{ kg/m}^3$  ranged from 0.055 to  $0.066 \text{ W/(mK)}$  depending on the size and thickness of wood shavings.

Heat transfer in a WS or CF mat occurs via solid conduction, gaseous conduction, convection, and radiation. The extent of solid conduction depends on the quantity of WS or CF in the mat, since these materials form heat bridges. It also depends on fiber alignments in the mat, because the  $k$ -value along the longitudinal direction is 2–3 times greater than that in the transverse direction [10]. Gaseous conduction depends on pore sizes in the mat. Fine pores like a cell lumen can be treated as quiescent air with a  $k$ -value of  $0.024 \text{ W/(mK)}$ , while coarse pores between the raw materials in the mat will be affected by air convection. Thermal radiation depends on the optical properties of the element surfaces. Although heat transfer mechanisms in closed-cell foam and fibrous insulation materials have been studied [2], there are few studies on these mechanisms in CF or WS mats in the literature.

This study investigated the  $k$ -value of CF mats and WS mats as a function of mat density. Mat density dependence in  $k$ -values was also investigated, with special emphasis on heat transfer in the coarse pores in the mat, by calculating the apparent  $k$ -value, which includes the effects of convection and radiation. The apparent  $k$ -value of coarse pores was determined by applying the rule of mixtures to two layer-arrangement models in which the layers were arranged parallel to and perpendicular to the direction of heat flow, respectively.

## Materials and methods

### Sample preparation

The raw material used for the CF test samples was a commercial CF material made from recycled newspapers

without any chemical agents. The CF, in its transportation package state, was passed through a dust collector a few times for fiberizing, and was adjusted to have a mat bulk density of approximately  $20 \text{ kg/m}^3$  prior to producing the test samples. The moisture content of the CF was about 10 %. Figure 1 shows the procedure for producing a test sample. In Step 1, the required mass of CF was uniformly sprinkled by hand in a metal forming box with walls 2 mm thick and an inner size of  $316 \times 316 \times 150$  (height) mm, which was inserted into a rigid glass wool frame measuring  $450 \times 450 \times 50$  mm that works as horizontal thermal insulation during the measurement of  $k$ -values. The bottom of the frame was equipped with a heat flow meter measuring  $300 \times 300 \times 0.7$  mm, which worked as a bottom plate to hold the mat. In Step 2, the mat was compressed a few times using a drop lid until the height of the mat was approximately 50 mm. In Step 3, the CF mat test sample measuring  $320 \times 320 \times 50$  mm was finished by carefully taking out the metal forming box. Test samples with a density of  $28\text{--}60 \text{ kg/m}^3$  were produced; one sample for every  $2 \text{ kg/m}^3$ , which resulted in 17 levels of density.

The raw material used for the WS test samples was Douglas fir [*Pseudotsuga menziesii* (Mirb.) Franco] wood shavings generated during commercial wood processing as waste material from the wooden frame members of houses. The moisture content and mat bulk density of the WS were 11 % and  $52 \text{ kg/m}^3$ , respectively. The average size of 50 randomly selected WS flakes was  $13.3 \times 14.8 \times 0.21$  mm. Test samples with densities of  $60\text{--}100 \text{ kg/m}^3$  were produced in a manner similar to the CF mats, with one sample for every  $2 \text{ kg/m}^3$ , which resulted in 21 levels of density.

### Measurement of $k$ -values

The heat flow meter method, as described in ASTM C518 [11], was employed. The sample mat was covered with another heat flow meter same as used for the bottom of the mat, then, the test sample sandwiched with two heat flow meters was inserted between upper and lower heat platens measuring  $450 \times 450$  mm. The temperature on both sides of the samples was measured using three sets of thermocouples. The temperature of the heat platens was set in one of two ways: either the upper platen was set at  $40 \text{ }^\circ\text{C}$  and the lower platen at  $20 \text{ }^\circ\text{C}$ , which generated a downward heat flow, or the opposite way around, which generated an upward heat flow.

Two replicate measurements, flipping the sample mat for each heat flow direction (i.e., four measurements in total), were conducted for each density level of each material. After confirming that the magnitude of heat flow had reached a constant (after 6–10 h depending on mat density), the  $k$ -value of the test sample at  $30 \text{ }^\circ\text{C}$  was calculated, using Eq. (1):

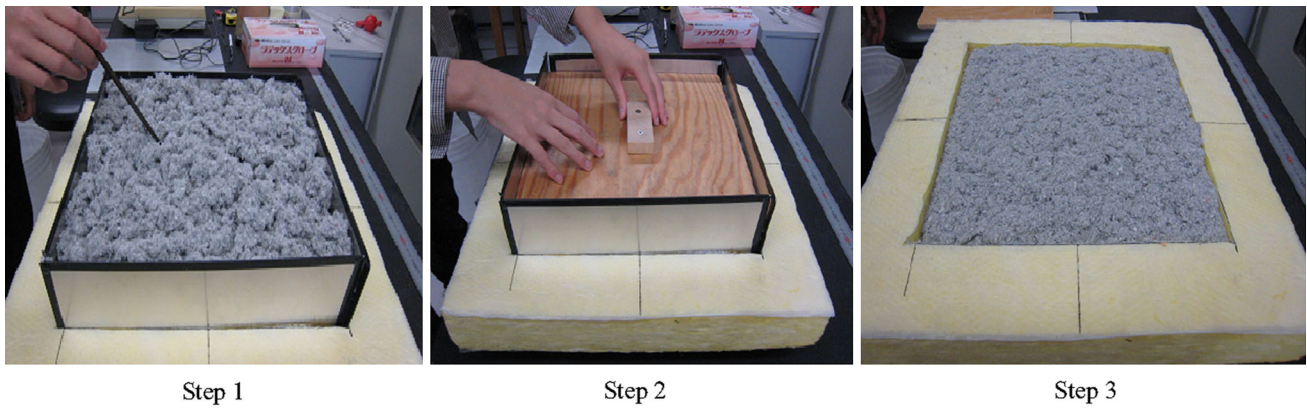


**Fig. 1** Procedure for producing a test sample

$$k = q_{av} \times d / \Delta T \text{ [W/(mK)],} \tag{1}$$

where  $q_{av}$  is the average heat flux ( $\text{W/m}^2$ ) measured at the upper and lower sides of the sample,  $d$  is the thickness of the mat sample (50 mm), and  $\Delta T$  is the temperature difference (K) between upper and lower surfaces of the sample.

**Theory**

Kollmann [10] proposed a heat transfer model of wood in which the direction of heat flow was either parallel or perpendicular to the two layers of the material (cell wall and cell lumen). Shida and Okuma [12] expanded Kollmann’s model from two elements to four elements (cell wall substance, adhesive, absorbed moisture, and air in the empty spaces) in order to theoretically investigate the  $k$ -value of particleboards. To examine heat transfer in wood-based mats, the present study replaced those elements with cell wall, absorbed moisture, fine pores (cell lumen), and coarse pores between the raw materials in the mat.

Figure 2 shows a series model and a parallel model consisting of the above four elements. The  $k$ -value of the series model is minimized ( $k_{min}$ ) because the element with minimum thermal resistance is dominant, while that of the parallel model is maximized ( $k_{max}$ ) because the total heat flow is determined by summing the heat flow in each element. Theoretically, the  $k$ -value of the mat lies between  $k_{min}$  and  $k_{max}$ , as expressed by Eq. (2), with a factor  $Z$  that indicates the relative importance of the parallel model ( $0 \leq Z \leq 1$ ).

$$k = Z \times k_{max} + (1-Z) \times k_{min} \tag{2}$$

The value of  $k_{min}$  and  $k_{max}$  is calculated by Eqs. (3) and (4), respectively, on the basis of the rule of mixtures as it applies to laminated materials:

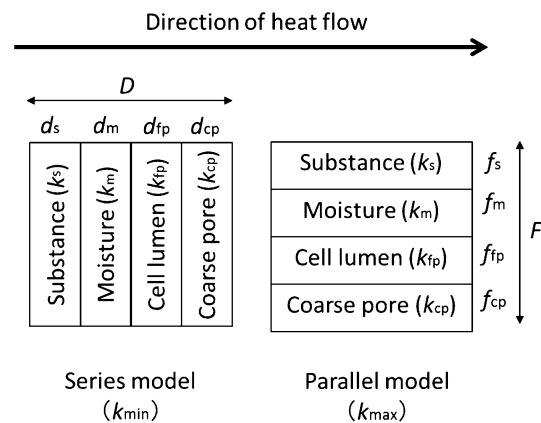


**Fig. 2** Series and parallel models including the four elements used for modeling heat transfer in cellulose fiber (CF) and wood shavings (WS) mats

$$k_{min} = \frac{D}{\sum(\frac{d}{k})} = \frac{V}{\frac{V_s}{k_s} + \frac{V_m}{k_m} + \frac{V_{fp}}{k_{fp}} + \frac{V_{cp}}{k_{cp}}} \tag{3}$$

$$k_{max} = \frac{\sum(f \times k)}{F} = \frac{V_s \times k_s + V_m \times k_m + V_{fp} \times k_{fp} + V_{cp} \times k_{cp}}{V} \tag{4}$$

where  $D$  and  $d$  are the length of the series model and of each element, respectively,  $V$  indicates the volume of the model or of each element, and  $F$  and  $f$  indicate the width of the parallel model and of each element, respectively. The suffixes  $s$ ,  $m$ ,  $fp$ , and  $cp$  represent cell wall, absorbed moisture, fine pores (cell lumen), and coarse pores, respectively.

**Results**

**Density dependence in  $k$ -values**

Figure 3 shows the relationships between mat density and  $k$ -values of the two types of mats. The data are plotted

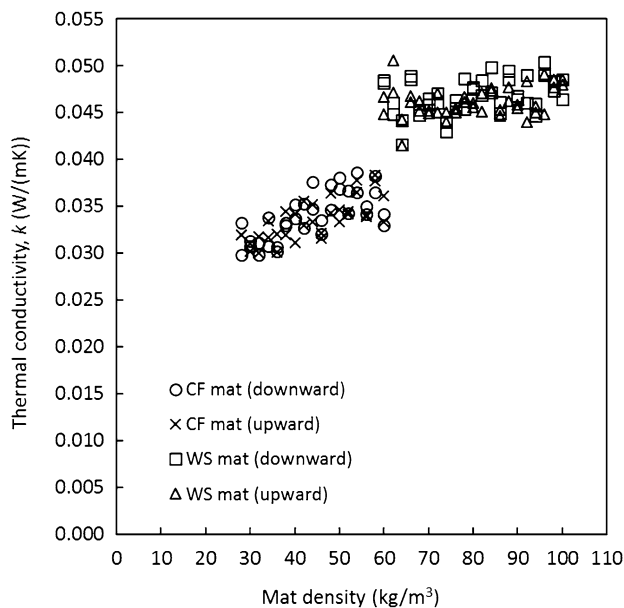


**Fig. 3** Relationships between mat density and thermal conductivity, CF cellulose fiber, WS wood shavings

separately according to heat flow direction. For CF mats, a statistically significant correlation ( $P < 0.01$ ) was found for both heat flow directions, and the following regression equations were obtained for upward and downward heat flux, respectively.

$$y = 1.81 \times 10^{-4}x + 0.0260 \quad (R^2 = 0.486) \quad (5)$$

$$y = 1.64 \times 10^{-4}x + 0.0263 \quad (R^2 = 0.537) \quad (6)$$

Statistical analysis of the difference between two regression equations showed that there was no significant difference between Eqs. (5) and (6). This indicates that the  $k$ -value of CF mats is not affected by heat flow direction, according to the best possible measurement accuracy in this experiment. In contrast, WS mats showed poor correlation between density and  $k$ -value. There was a statistically significant correlation ( $P < 0.05$ ) in the downward heat flow (Eq. 7), but not in the upward heat flow.

$$y = 5.35 \times 10^{-5}x + 0.042 \quad (R^2 = 0.118) \quad (7)$$

A detailed examination of the significance of the differences between the average  $k$ -values for the two heat flow directions was conducted for two ranges of mat density: the lower half (60–80 kg/m<sup>3</sup>) and the upper half (80–100 kg/m<sup>3</sup>). The results revealed that there was no significant difference in the lower half of mat density, but there was a small difference of 2 % (upward < downward) in the upper half.

Based on these results, mat density dependence in  $k$ -values can be discussed without considering heat flow directions. Equations (8) and (9) show the regression

equations obtained when ignoring heat flow direction for CF mats and WS mats, respectively.

$$y = 1.73 \times 10^{-4}x + 0.0262 \quad (R^2 = 0.502) \quad (8)$$

$$y = 4.55 \times 10^{-5}x + 0.0428 \quad (R^2 = 0.095) \quad (9)$$

From Eq. (8), the  $k$ -value of the CF mat was found to increase by approximately 5 % with every 10 kg/m<sup>3</sup> increase in mat density. This suggests that the number of heat bridges (which facilitate heat transfer by conduction) formed by fibers increase with increasing mat density. Closer examination of Fig. 3, however, reveals for densities of more than 50 kg/m<sup>3</sup>, the  $k$ -value tended to level off. Further examination of this issue will require more experimental data with a greater range of mat densities.

Although a significant correlation ( $P < 0.01$ ) was also found for the WS mats, the coefficient of correlation was very low. The density dependence of the  $k$ -values of WS mats is therefore much lower than that of CF mats; in fact the slope of the regression equation is approximately four times greater for CF mats. This can be explained by the size distribution of coarse pores in WS mats, since lower density mats tend to have larger coarse pores in which greater convective heat transfer may occur, resulting in higher  $k$ -values.

### Difference in $k$ -values between CF and WS mats

In this experiment, we examined both CF and WS mats with a density of 60 kg/m<sup>3</sup>. Figure 4 compares the appearance of the two kinds of mat at that density. The  $k$ -values obtained from the regression equations for CF and WS mats with a density of 60 kg/m<sup>3</sup> are 0.0364 and 0.0456 W/(mK), respectively. Thus the  $k$ -value of the WS mat was 1.25 times higher than that of the CF mat. Assuming that the CF and WS materials themselves have the same solid  $k$ -value, and therefore that heat transfer via solid conduction occurs to the same degree when mat density is equal, the above difference in  $k$ -values is presumably caused by the difference in heat transfer through coarse pores.

## Discussion

### Calculation of $k$ -values for coarse pores ( $k_{cp}$ )

Kollmann [10] indicated that the factor  $Z$  in Eq. (2) characterizes the network of heat bridges within the structure of wood and wood-based materials, and that the value of  $Z$  does not depend upon density when the two elements of cell wall and cell lumen are used in the model. Shida and Okuma [12] concluded that  $Z$  is a constant value for



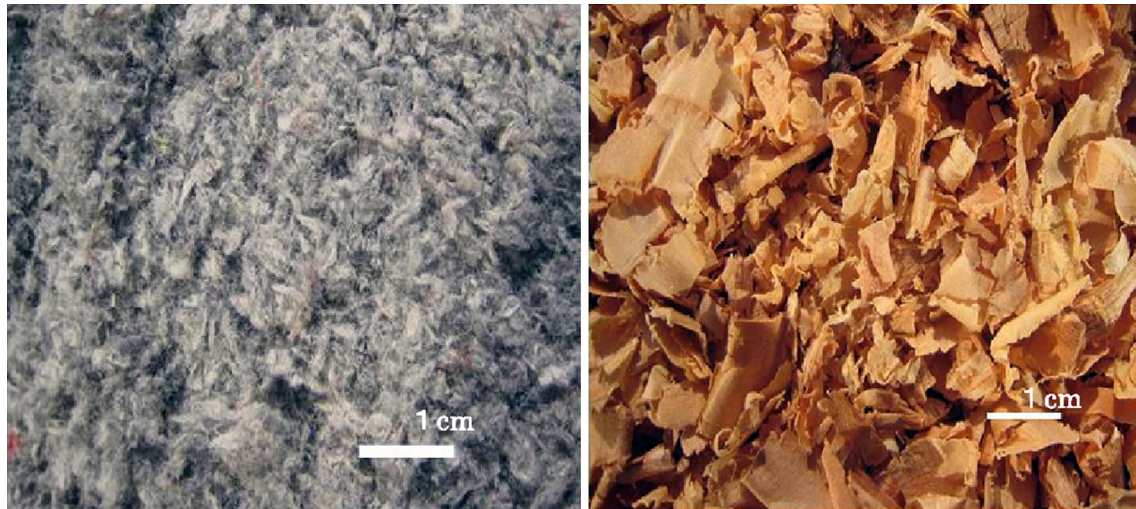


**Fig. 4** Surface appearance of a CF mat (*left*) and a WS mat (*right*) with a density of  $60 \text{ kg/m}^3$

particleboards with densities of  $400\text{--}900 \text{ kg/m}^3$ , when the aforementioned four elements are used in the model. From these findings, there is a possibility that CF and WS mats also have constant  $Z$  values for certain density ranges. In the present study, the  $k$ -value of coarse pores ( $k_{cp}$ ) in CF and WS mats was determined using the following calculation steps.

Step 1: Calculation of  $k_{min}$  and  $k_{max}$

Equations (3) and (4) require the volume of each element ( $V_s$ ,  $V_m$ ,  $V_{fp}$ , and  $V_{cp}$ ) and their total volume ( $V$ ). They are calculated by Eqs. (10–14), where  $W$  and  $r$  indicate the mass and density of a mat with the corresponding moisture content (MC in %), and  $W_s$  and  $r_s$  are the same for the cell wall and  $W_m$  and  $r_m$  for absorbed moisture, and  $r_a$  indicates the apparent air-dry density of CF or WS with the corresponding moisture content (MC in %).

$$V = \frac{W}{r} = \frac{W_s + W_m}{r} = \frac{W_s \left(1 + \frac{MC}{100}\right)}{r} \quad (10)$$

$$V_s = \frac{W_s}{r_s} \quad (11)$$

$$V_m = \frac{W_m}{r_m} = W_s \times \frac{MC}{100} \times \frac{1}{r_m} \quad (12)$$

$$V_{fp} = \frac{W_s \left(1 + \frac{MC}{100}\right)}{r_a} - W_s \left(\frac{1}{r_s} + \frac{MC}{100 \times r_m}\right) \quad (13)$$

$$V_{cp} = \frac{W_s + W_m}{r} - \frac{W_s + W_m}{r_a} = \frac{W_s \left(1 + \frac{MC}{100}\right)}{r} - \frac{W_s \left(1 + \frac{MC}{100}\right)}{r_a} \quad (14)$$

When substituting Eqs. (10–14) into Eqs. (3) and (4), and plugging in the values shown in Table 1, then,  $k_{min}$  and  $k_{max}$  are expressed as a function of  $k_{cp}$ .

The volume of each element depends on mat density;  $V_s$  and  $V_m$  increase linearly with increasing mat density. So does  $V_{fp}$  unless cell lumens collapse. On the other hand,  $V_{cp}$  decreases with increasing mat density. Table 2 lists the volume percent of each element for CF and WS mats with their minimum and maximum mat densities employed in this experiment.

Step 2: Iterative computation

After completing Step 1, when substituting Eqs. (3) and (4) into Eq. (2), the  $k$ -value of the mat is determined by two parameters,  $k_{cp}$  and  $Z$ . In other words, the value of  $Z$  is calculated from  $k_{cp}$  and the  $k$ -value of the mat. In the present numerical experiments, an optimum value for  $k_{cp}$  was calculated on the assumption that the mats have a constant  $Z$  value for each half (upper and lower) of the range of mat densities. The mat  $k$ -value used for the calculation was obtained from the regression equations: Eq. (8) was used for CF mats, and not Eq. (9) but Eq. (15) was used for WS mats.

$$y = 2.35 \times 10^{-6}x^2 - 3.31 \times 10^{-4}x + 0.0575 \quad (15)$$

$$(R^2 = 0.124)$$

The calculation was implemented for every  $2 \text{ kg/m}^3$  step in mat density for the lower half the density range ( $28\text{--}44 \text{ kg/m}^3$  for CF mats and  $60\text{--}80 \text{ kg/m}^3$  for WS mats) and the upper half ( $44\text{--}60 \text{ kg/m}^3$  for CF mats and  $80\text{--}100 \text{ kg/m}^3$  for WS mats) using a given value for parameter  $k_{cp}$  in the range specified below. The mean value of  $Z$  and its coefficient of variance (COV) were then calculated.

Iterative computation was conducted, changing the value of  $k_{cp}$  by  $0.001 \text{ W/(mK)}$  from  $0.022$  to  $0.030 \text{ W/(mK)}$  for CF mats and from  $0.035$  to  $0.049 \text{ W/(mK)}$  for WS mats. Based on the assumption that the mats have a

**Table 1** Density and  $k$ -value of each element used for determining  $k_{min}$  and  $k_{max}$

Elements	Properties	CF mats	WS mats
Cell wall	Density, $r_s$ (kg/m <sup>3</sup> )	1550	1500
	$k$ -Value, $k_s$ [W/(mK)] <sup>a</sup>	0.54	0.54
Absorbed moisture	Density, $r_m$ (kg/m <sup>3</sup> )	1100	1100
	$k$ -Value, $k_m$ [W/(mK)]	0.60	0.60
Fine pores (cell lumen)	Density (kg/m <sup>3</sup> )	Negligible	Negligible
	$k$ -Value, $k_{fp}$ [W/(mK)]	0.025	0.025
Coarse pores	Density (kg/m <sup>3</sup> )	Negligible	Negligible
	$k$ -Value, $k_{cp}$ [W/(mK)]	Parameter	Parameter
Raw materials	Apparent air-dry density, $r_a$ (kg/m <sup>3</sup> )	400	380
	Moisture content (%)	10	11

<sup>a</sup> Average of  $k$ -value parallel to and perpendicular to the cell wall longitudinal direction [13]

**Table 2** Volume percent of elements composing the mat

Elements	CF mats		WS mats	
	30 kg/m <sup>3</sup>	60 kg/m <sup>3</sup>	60 kg/m <sup>3</sup>	100 kg/m <sup>3</sup>
Cell wall, $V_s$ (%)	1.8	3.5	3.6	6.0
Absorbed moisture, $V_m$ (%)	0.2	0.5	0.5	0.9
Fine pores (cell lumen), $V_{fp}$ (%)	5.5	11.0	11.6	19.4
Coarse pores, $V_{cp}$ (%)	92.5	85.0	84.2	73.7
Mat, $V$ (%)	100.0	100.0	100.0	100.0

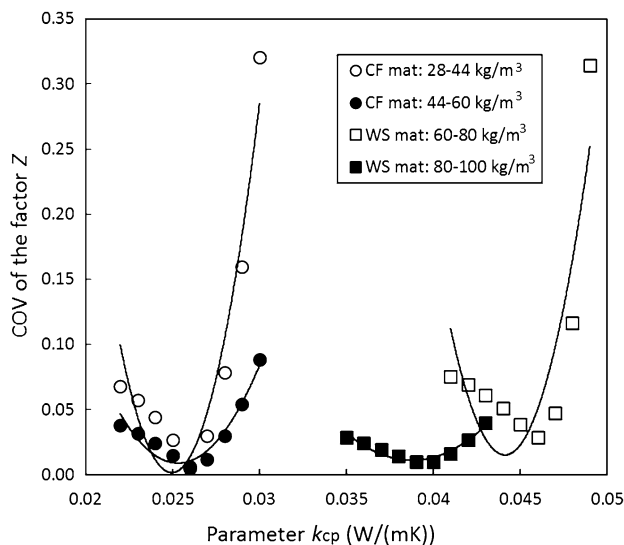


**Fig. 5** Relationships between the parameter  $k_{cp}$  and the coefficient of variance (COV) of factor Z

constant Z value, the optimum value of  $k_{cp}$  is the one that yields a local minimum COV for Z.

**Comparison of  $k_{cp}$**

The results of the iterative computations are shown in Fig. 5, as the relationships between  $k_{cp}$  and the COV of

Z. Although the behavior of the COV depended on mat type and density range, a local minimal value was identifiable for all four cases. Regression curves with a completing square were calculated and they are as follows:

CF mat (lower half of density range):

$$y = 1.12 \times 10^4(x - 0.0250)^2 + 0.0017 \quad (R^2 = 0.925) \quad (16)$$

CF mat (upper half) :

$$y = 3.43 \times 10^3(x - 0.0253)^2 + 0.0088 \quad (R^2 = 0.937) \quad (17)$$

WS mat (lower half) :

$$y = 9.96 \times 10^3(x - 0.0441)^2 + 0.0152 \quad (R^2 = 0.785) \quad (18)$$

WS mat (upper half) :

$$y = 1.48 \times 10^3(x - 0.0388)^2 + 0.0113 \quad (R^2 = 0.927) \quad (19)$$

Table 3 lists the optimum  $k_{cp}$  values obtained from the experimental plots and regression equations, and the values of Z. The  $k_{cp}$  values from the regression equations were almost the same as or slightly smaller than those from the experimental plots. For CF mats, the  $k_{cp}$  value obtained was 0.025–0.026 W/(mK), which was almost the same as the  $k$ -value of quiescent air [0.024 W/(mK)]. This indicates that the coarse pores in CF mats within this density range are small enough to preclude any convective heat transfer through the air. In contrast, the  $k_{cp}$  value obtained for WS mats differed depending on mat density. The  $k_{cp}$  value for

**Table 3** Comparisons of  $k_{cp}$  and  $Z$  values for CF mats and WS mats

	$k_{cp}$ [W/(mK)]	$Z$
CF mats		
28–44 kg/m <sup>3</sup>	0.026 (0.025)	0.47
44–60 kg/m <sup>3</sup>	0.026 (0.025)	0.46
WS mats		
60–80 kg/m <sup>3</sup>	0.046 (0.044)	0.22
80–100 kg/m <sup>3</sup>	0.039 (0.039)	0.31
WSBIP		
80–120 kg/m <sup>3</sup>	0.045 (0.045)	0.61

Values in parenthesis were obtained from regression curves

WSBIP wood shaving binderless insulation panel [14]

the lower half of the density range (60–80 kg/m<sup>3</sup>) was 1.8 times greater than that of quiescent air. This suggests that coarse pores between flakes form some continuous gaps along heat flow direction resulting in convective heat transfer. However, the value for the upper half (80–100 kg/m<sup>3</sup>) was 0.039 W/(mK), smaller than that in the lower half of the density range. This indicates that the size of the coarse pores decrease with increasing mat density, which leads to a coarse pore structure that allows less convective heat transfer. Also, the fact that the  $k$ -values of WS mats are less density dependent than those of CF mats can be explained by the difference in  $k_{cp}$  between the lower and upper halves of the mat density range, because the decrease in  $k_{cp}$  contributes to the lowering of mat thermal conductivity in a way that balances the increasing number of heat bridges as mat density increases.

Table 3 also shows reference values for WS binderless insulation panels (WSBIPs). Sekino and Yamaguchi [14] reported that the  $k$ -value of a WSBIP with a mat density of 100 kg/m<sup>3</sup> was 0.066 W/(mK), and its  $k_{cp}$  was 0.045 W/(mK). These values are higher than those obtained for WS mats in the present study. This is because WSBIPs are manufactured using an extrusion mat-forming method that tends to face the longitudinal direction of the wood in the direction of heat flow through the panel thickness: the  $k$ -value of the longitudinal direction of wood is 2–3 times greater than its perpendicular. The value of  $Z$  obtained for WSBIPs was approximately 2–3 times greater than that for WS mats. This is consistent with the fact that the factor  $Z$  in Eq. (2) indicates the relative importance of the parallel model in determining the maximum  $k$ -value in the mat.

**Acknowledgments** This research was partly supported by a Grant-in-Aid for Scientific Research (C) (No. 26450223), for which the author is grateful.

## References

1. Sekino N (2015) Characteristics of wood-based insulation materials (in Japanese). *Jutaku-to-Mokuzai* (Japan Housing and Wood Technology Center) 38(3):6–9
2. Kwon J, Jang C, Jung H, Song T (2009) Effective thermal conductivity of various filling materials for vacuum insulation panels. *Int J Heat Mass Transfer* 52:5525–5532
3. Binici H, Eken M, Dolaz M, Aksogan O, Kara M (2014) An environmentally friendly thermal insulation material from sunflower stalk, textile waste and stubble fibers. *Constr Build Mater* 51:24–33
4. Zhou X, Zheng F, Li H, Lu C (2010) An environment-friendly thermal insulation materials from cotton stalk fibers. *Energy Build* 42:1070–1074
5. Yamauchi H, Sasaki H, Ma LF, Xu H, Pulido OR (2001) Design and production of heated floor panels from wood barks. In: *Proceedings of symposium on utilization of agricultural and forestry residues*, Nanjing, pp 72–76
6. Kawamura Y, Sekino N, Yamauchi H (2004) Binder-less wood chip insulation panel for building II. Effect of chip thickness and panel density on thermal conductivity and resistance against falling impact (in Japanese). *Mokuzai Gakkaishi* 50:228–235
7. Kawamura Y, Sekino N, Yamauchi H (2004) Binder-less wood chip insulation panel for building III. Effect of raw material density on thermal conductivity and resistance against falling impact (in Japanese). *Mokuzai Gakkaishi* 50:397–403
8. Sekino N, Kawamura Y, Yamauchi H (2006) Binder-less wood chip insulation panel for building IV. Heat storage capacity of full-scale thick panels manufactured using wood shavings (in Japanese). *Mokuzai Gakkaishi* 51:380–386
9. Sekino N, Yamauchi G (2009) Fire safety of wooden walls filled with binder-less wood shavings insulation panels. *PRO Ligno* 5(2):23–32
10. Kollmann FP (1968) *Principles of wood science and technology, I. Solid wood*. Springer-Verlag, Berlin, pp 247–249
11. ASTM C518 (1991) Standard test method for steady-state heat flux measurements and thermal transmission properties by means of the heat flow meter apparatus. ASTM International, West Conshohocken
12. Shida S, Okuma M (1981) The effects of the apparent specific gravity on thermal conductivity of particleboard (in Japanese). *Mokuzai Gakkaishi* 27:775–781
13. Koshijima T, Sugihara H, Hamada R, Fukuyama M, Huse G (1979) *Kiso Mokuzaikougaku* (in Japanese). Futaba-Shoten, Osaka, p 87
14. Sekino N, Yamaguchi K (2013) Mechanisms behind better thermal insulation capacity of carbonized binder-less wood shaving insulation panels—investigation from apparent thermal conductivity of coarse pore (in Japanese). *Wood Carboniz Res* 9(2):68–74